Autonomous Mobility Improvements of Hybrid Electric 4x4 with Controllable Power Transmitting Unit

Vladimir Vantsevich¹ and Jesse Paldan¹

¹ The University of Alabama at Birmingham, Birmingham, AL 35294, U.S.A vantsevi@uab.edu jpaldan@uab.edu

Abstract. Bringing vehicle autonomy to the level of its driveline system means that the autonomous vehicle has the capability to autonomously control the distribution of power between its driving wheels. A vehicle can therefore improve mobility by autonomously redistributing wheel power. For this implementation, vehicle mobility must first be quantified by suitable mobility indices, derived from vehicle dynamics, to numerically show a wheel or vehicle is close to immobilization as well as evaluate the effect of mobility improvements on the vehicle velocity. A velocity-based mobility index combines wheel traction with velocity to maximize effectiveness of movement. Computer simulations demonstrate the potential to improve velocity by optimizing vehicle mobility of a 4x4 vehicle with a hybrid electric power transmitting unit.

Keywords: Vehicle Mobility, Driveline Systems, Vehicle Autonomy

1 Introduction

Using autonomous ground vehicles (AGVs) on uncertain terrain brings a need for the vehicle to evaluate its mobility on a moment-to-moment basis. This presents a challenge since traditionally mobility has been evaluated on a go or no-go basis. In order to make use of power redistribution for mobility, the vehicle must be able to use quantitative evaluations of its mobility using available measurements of its current conditions in order to pick the most optimal strategy. Mobility metrics have been created for mobile robots to assist designers to quantify performance and compare different systems [1, 2]. Development of next-generation mobility models includes interest in giving intelligent vehicles and robots better tools for mobility assessment, decision making, and operational planning [3]. Recommendations for next-generation mobility models include being physics-based, capable of quantitative assessment, applicable to all terrain, and readily measurable [4].

In this paper, a mathematical model of a 4x4 vehicle with a configurable hybrid electric driveline is used as a framework for a study in autonomous mobility improvements. A hybrid electric power splitting device allows control over the balance of power distribution between the front and rear wheels. Two sets of indices are examined for quantifying the vehicle mobility: a wheel/vehicle mobility index based on individual

wheel force distribution, and a new velocity-based index which combines the effects of velocity and slippage of the vehicle.

2 Vehicle Dynamics for Mobility Analysis

To establish the effect of the power distribution on mobility and velocity, the interdependence of forces, slippage, and velocity is first discussed. Eq. (1) is the longitudinal forces which influence the straight line movement of a vehicle with four driving wheels:

$$F_{x\Sigma} = \sum_{i=1}^{4} F_{xi}^{\prime(i)} = \sum_{i=1}^{4} R_{xi}^{\prime(i)} + F_d \pm F_a + D_a \pm W_a \sin \theta_g \tag{1}$$

In Eq. (1), the right side of the equation is resistance to motion. The total rolling resistance is made up of the sum of rolling resistance forces at each wheel, including the left (R'_{xi}) and right (R''_{xi}) sides; signs '(") are for the right and left wheels. Inertial force from acceleration F_a , drawbar pull F_d , air drag D_a , and the gravity force from the vehicle weight W_a on slope θ_g also contribute to (or reduce) resistance. The total circumferential force, $F_{x\Sigma}$, is the sum of each wheel's circumferential force $F_{xi}^{'(")}$; these forces come from the applied wheel torques. The total circumferential force can be computed if the resistance to motion is known, but not the distribution of individual forces $F_{xi}^{'(")}$. These individual circumferential forces at the drive axles depend on the characteristics of the driveline system, as the driveline system determines the distribution of power between the driving wheels. The driveline system imposes constraints on the distribution of wheel forces and on the linear and angular velocities.

The vehicle's linear velocity drops from V_a to V_x when $F_{x\Sigma} > 0$. The velocity drop can be characterized by a slippage factor $s_{\delta a}$ that is introduced as the generalized slippage of the vehicle [5].

$$s_{\delta a} = \frac{v_a - v_x}{v_a} \tag{2}$$

$$V_x = V_a (1 - s_{\delta a}) \tag{3}$$

 V_a here is the theoretical linear velocity of the vehicle without slip. Velocity V_a is defined by the following expression [5]:

$$V_a = \omega_0 r_a^0 \tag{4}$$

where r_a^0 is the generalized rolling radius of the vehicle in the driven mode reduced to the input shaft of the transfer case. ω_0 is the rotation speed of the transfer case input shaft. Hence, the physical meaning of Eq. (4) is that the theoretical velocity is the linear velocity of an equivalent single wheel that rotates with rotational velocity ω_0 and has a rolling radius in the driven mode given by r_a^0 .

Without any connection to the vehicle frame, the wheels would be able to move independently and each would have a velocity V_{ti} defined by Eq. (5):

$$V_{ti} = \omega_{0i} r_{ai}^{0} = \frac{\omega_{0}}{u_{i}} r_{ai}^{0}, i = 1, n$$
 (5)

where i is the drive axle number, i=1,n. ω_{0i} is the angular velocity of the single equivalent wheel of a drive axle, i.e., the rotational velocity of the interaxle differential that is installed between the right and left wheels of the axle. r_{ai}^0 is the generalized rolling radius of the axle in the driven mode. u_i is the final drive gear ratio from each axle to the transfer case. The actual velocity of the vehicle can be expressed in terms of the theoretical velocities of the wheels and the generalized tire slippages of the axles, $s_{\delta ai}$:

$$V_x = V_{ti}(1 - s_{\delta ai}), i = 1, n$$
 (6)

Because they are connected by the vehicle frame, each wheel center, however, must move with the same linear velocity, V_a . When the velocities V_{ti} and V_a differ, this difference is referred to as a kinematic discrepancy. Kinematic discrepancy for each axle i is as follows:

$$m_{Hi} = \frac{V_{ti} - V_a}{V_{ti}}, i = 1, n \tag{7}$$

After substituting Eq. (4) and Eq. (5) in Eq. (7), m_{Hi} can be written as

$$m_{Hi} = 1 - r_a^0 \frac{u_i}{r_{ai}^0}, i = 1, n \tag{8}$$

When the total resistance to movement is close to zero, the relation between the circumferential wheel force, F_x , and the slippage, which is equal to the kinematic discrepancy factor in this mode of travel, can be accepted as a linear function [5]

$$F_{xi} = K_{ai} m_{Hi} = K_{ai} \left(1 - r_a^0 \frac{u_i}{r_{o,i}^0} \right), i = 1, n$$
 (9)

here, K_{ai} is the longitudinal stiffness of an equivalent wheel of an axle determined by the longitudinal stiffness factors of the left and right wheels of the axle. Since $F_{x\Sigma} \rightarrow 0$, then the sum of the axle torques, T_{ai} , reduced to the input shaft of the transfer case is equal to zero:

$$\sum_{i=1}^{n} \frac{T_{ai}}{u_i} = \sum_{i=1}^{n} \frac{F_{xi} r_{ai}^0}{u_i} = 0 , i = 1, n$$
 (10)

The generalized rolling radius of the vehicle in the driven mode r_a^0 can be determined after substituting Eq. (9) in Eq. (10):

$$r_a^0 = (\sum_{i=1}^n K_{ai} r_{ai}^0 / u_i) (\sum_{i=1}^n K_{ai})^{-1}, i = 1, n$$
(11)

Using Eq. (11) and Eq. (8), the kinematic discrepancy of the *i*-th axle of the vehicle is written as follows:

$$m_{Hi} = 1 - \frac{u_i}{r_{ai}^0} \frac{\sum_{i=1}^n K_{ai} r_{ai}^0 / u_i}{\sum_{i=1}^n K_{ai}}, i = 1, n$$
 (12)

The kinematic discrepancy factors therefore depend on the parameters in the right side of Eq. (12): the gear ratios u_i from the transfer case to the wheels, the rolling radii in

the driven mode r_{ai}^0 and the longitudinal stiffnesses K_{ai} . This becomes useful for control since the kinematic discrepancies are closely related to the slippage and velocity. If Eq. (3) and Eq. (6) are substituted into Eq. (7), the following equation is derived to relate generalized axle slippages to the generalized vehicle slippage:

$$s_{\delta i} = m_{Hi} + (1 - m_{Hi}) s_{\delta ai}, i = 1, n$$
 (13)

With a symmetrical open differential splitting power between the left and right wheels of an axle, the individual tire slippages are related to the generalized axle slippage by

$$s_{\delta ai} = 1 - \frac{\left(r_{wi}^{0"} + r_{wi}^{0'}\right)\left(1 - s_{\delta i}^{"}\right)\left(1 - s_{\delta i}^{'}\right)}{r_{wi}^{0'}\left(1 - s_{\delta i}^{'}\right) + r_{wi}^{0"}\left(1 - s_{\delta i}^{'}\right)}, i = 1, n$$
(14)

where $r_{wi}^{o'(\prime\prime)}$ are the individual tire rolling radii in the driven mode. The tire slippage is linked to circumferential force F_x ; wheel traction functions for relating the two on soft soil are nonlinear and derived from a tire-soil model or found experimentally. Eq. (15) is a function for the tire slip widely used in technical literature.

$$F_{xi}^{\prime(\prime\prime)} = \mu_{pxi}^{\prime(\prime\prime)} R_{zi}^{\prime(\prime\prime)} \left(1 - e^{-k_i^{\prime(\prime\prime)} s_{\delta i}^{\prime(\prime\prime)}} \right), i = 1, n$$
 (15)

 μ_{px} is the peak friction coefficient of the terrain, defined as the ratio of maximum attainable wheel traction force to normal load. Therefore, $\mu_{px}R_z$ is the maximum circumferential force under current terrain conditions; k is an empirical factor that depends on properties of the tire and surface. From Eq. (1), values of $F_{xi}^{\prime(\prime\prime)}$ in Eq. (15) must add up to $F_{x\Sigma}$ defined by the vehicle motion resistance. The distribution of forces among the wheels is influenced by slippages and kinematic discrepancies in Eq. (13).

2.1 Hybrid Electric Power Transmitting Unit for Mobility Optimization

Control over the vehicle's power split is achieved here through the addition of a controllable planetary gear set in the vehicle's driveline, installed between the transfer case and an axle (Fig. 1). The planetary gear set in this Hybrid Electric-Power Transmitting Unit (HE-PTU) has three elements connected to its input/output shafts: the ring gear, sun gear, and planet carrier [6]. The sun gear and carrier are the input and output shafts of the HE-PTU, with torques T_{in} and T_{out} . Attached to the ring gear is an eddy current brake which draws power from the vehicle's hybrid electric power system and exerts an additional torque T_B on its shaft.

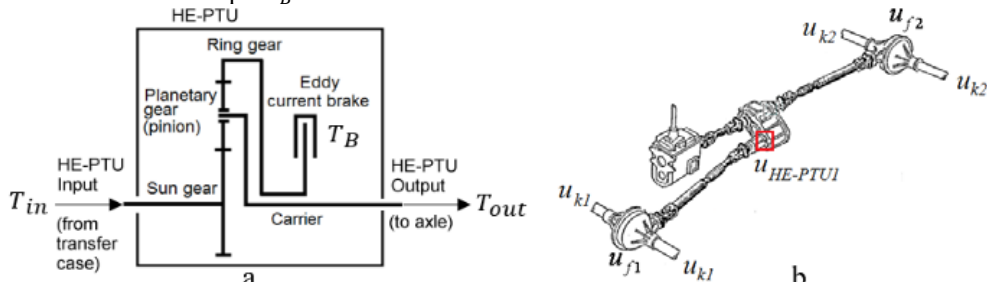


Fig. 1: a) HE-PTU Diagram, b) position of HE-PTU in 4x4 driveline layout

A planetary gear set has a gear ratio K which is defined as the ratio of the number of teeth on the ring gear to that of the sun gear. For the input/output configuration in Fig. 1, the gear ratio between the input and output when the third element is locked is 1 + K; the torque T_B^{max} to fully lock the ring gear would be equal to Eq. (16).

$$T_B^{max} = T_{in}K = T_{out} \frac{\kappa}{1+\kappa}$$
 (16).

This means that if the eddy current brake were applying the maximum torque T_B^{max} necessary to stop the ring gear, the gear ratio between the input and output would be $u_{HE-PTU}^{max} = 1 + K$. If the braking torque is released, lowering torque T_B from T_B^{max} , the gear ratio decreases from this maximum value. Therefore, the HE-PTU provides a variable gear ratio u_{HE-PTU} expressed by Eq. (17)

$$u_{HE-PTU} = u_{HE-PTU}^{max} \frac{T_{B}}{T_{B}^{max}} = \frac{(1+K)}{K} \frac{T_{B}}{T_{in}} = \frac{(1+K)^{2}}{K} \frac{T_{B}}{T_{out}}$$
(17)

By varying the eddy current brake torque and thus controlling u_{HE-PTU} , the vehicle generalized rolling radius (Eq. (11)) and kinematic discrepancies (Eq. (12)) are also controllable.

3 Indices for Mobility Evaluation

Mobility requires a vehicle to have a capability to move from place to place in terrain conditions while retaining its ability to perform effectively a payload transportation task. In this regard, to maximize the productivity of the transportation task, the vehicle also needs to be able to operate with maximum mobility. Thus, an approach to the wheel and vehicle mobility assessment needs to combine and analyze the wheel traction with the velocity to increase and then to maximize the effectiveness of the movement, i.e. to maximize mobility. Accordingly, the objective function for the maximization of vehicle mobility should contain the circumferential wheel forces, F_x , and actual velocity, V_x . Therefore, the dependencies of the components of F_x and V_x should be established. In particular, tire slippage influences both the circumferential force and the velocity.

3.1 Wheel Mobility Index

Optimizing individual tire slippages and, thus, circumferential wheel forces requires a vehicle mobility index or several indices that allow for assessing the contribution and establishing boundaries that each individual driving wheel provides and imposes on the vehicle mobility. At the same time, the mathematical appearance of the indices should be light enough to make their components easily determined and, thus, provide a potential for real-time control applications. The first set of wheel mobility indices that can satisfy these requirements is the Wheel Mobility Index and Vehicle Mobility Index [7]:

$$WMI_{\mu i} = 1 - \frac{F_x}{F_{x \, max}} = 1 - \left(\frac{\mu_{xi}}{\mu_{pxi}}\right)$$
 (18)

$$VMI_{\mu} = \sum_{i=1}^{n} \frac{WMI'_{\mu i}^{(\prime\prime)}}{2n} = 1 - \frac{1}{2n} \sum_{i=1}^{n} \frac{F_{xi}^{\prime(\prime\prime)}}{F_{xi}^{max\prime(\prime\prime)}} = 1 - \frac{1}{2n} \sum_{i=1}^{n} \frac{\mu_{xi}^{\prime(\prime\prime)}}{\mu_{yxi}^{\prime(\prime\prime)}}$$
(19)

here, $F_{xi}^{max \ \prime(\prime\prime)}$ is the maximum circumferential force determined by the gripping properties of tires, $F_{xi}^{max \ \prime(\prime\prime)} = \mu_{pxi}^{\prime(\prime\prime)} R_{zi}^{\prime(\prime\prime)}$, $\mu_{pxi}^{\prime(\prime\prime)}$ is the peak friction coefficient, $R_{zi}^{\prime(\prime\prime)}$ is the wheel normal reaction, and $F_{xi}^{\prime(\prime\prime)}$ is the current circumferential force of a wheel that is linked to the current friction coefficient, $\mu_{xi}^{\prime(\prime\prime)}$, where $\mu_{xi}^{\prime(\prime\prime)} = F_{xi}^{\prime(\prime\prime)}/R_{zi}^{\prime(\prime\prime)}$. In this approach, vehicle mobility is estimated by an index, which counts the mo-

In this approach, vehicle mobility is estimated by an index, which counts the mobility indices of all wheels, i.e., the method values contributions of each and every wheel. The variables in Eq. (18) and Eq. (19) are able to be determined and estimated in real-time to assess how close the wheel or vehicle is to immobilization.

3.2 Velocity-based Index

The wheel and vehicle mobility assessment also needs to combine and analyze the wheel traction with the velocity. For this purpose, an index is needed to estimate the influence of the power split between the driving wheels on the effectiveness of vehicle movement, meaning the vehicle can move at a higher velocity on the same terrain than a vehicle with lower mobility potential. This Velocity-based Mobility Performance Index is derived in the following equations.

Eq. (11) puts the generalized rolling radius of the vehicle in terms of the individual axle generalized rolling radii in the driven mode, the longitudinal stiffness, and the gear ratios. With the HE-PTU installed, the variable gear ratios u_i are

$$u_i = u_{HE-PTUi} u_{fd} \tag{20}$$

where u_{fd} is the fixed final drive ratio. To examine the effect changing these gear ratios would have, first define a rolling radius r_{a*}^0 in which the variable gear ratios are equal and replaced with a fixed final drive ratio u_{fd} (making $u_{HE-PTU} = 1$):

$$r_{a*}^{0} = \frac{\sum_{i=1}^{n} K_{ai} r_{ai}^{0}}{u_{fd}(\sum_{i=1}^{4} K_{ai})} \tag{21}$$

Eq. (4) will also transform into Eq. (22), the theoretical linear velocity of the vehicle at $u_i = u_{fd}$.

$$V_{a*} = \omega_0 r_{a*}^0 \tag{22}$$

The Velocity-based Mobility Performance Index η_{vmp} is then defined by Eq. (23) [8].

$$\eta_{vmp} = \frac{V_x}{V_{xy}} \tag{23}$$

Eq. (23) provides an index that evaluates the influence of the power split on the vehicle mobility performance. Specifically, it integrates two concepts: the change in velocity from V_{a*} to V_a resulting from the change to the vehicle's generalized rolling radius in the driven mode and the change from V_a to V_x resulting from the slip ratio $S_{\delta a}$.

4 Computational Mobility Study

Computer simulations were conducted to study the evaluation of mobility on variable terrain conditions. Three different driveline configurations where mathematically modeled. These drivelines are:

- 1. Optimized: A hybrid electric driveline system with an HE-PTU installed between the transfer case and front axle. A computer optimization algorithm was used to find the optimal ratio u_{HE-PTU} which leads to optimal values of η_{vmp} , and therefore the greatest velocity improvement.
- 2. Conventional: A conventional mechanical driveline with all open differentials.
- 3. Non-optimized: The same hybrid electric configuration as the optimized case, but the gear ratio u_{HE-PTU} is held constant to match the gear ratio of case 2.

Three terrain conditions were modeled for the vehicle to traverse: deformable soil with properties matching Norfolk Sandy Loam, meadow, and an asphalt road. The terrain is a profile with a stochastic modeling of continuous changes in its peak friction coefficient and rolling resistance. Fig. 2 illustrates the terrain model that was applied to the vehicle motion simulation. The peak friction coefficient changes stochastically with smooth variations as well as more sudden drops, modeling a terrain with variable soil quality, moisture content, etc. which impact the tire's peak friction coefficient. The left and right wheels have separate tracks with different patterns.

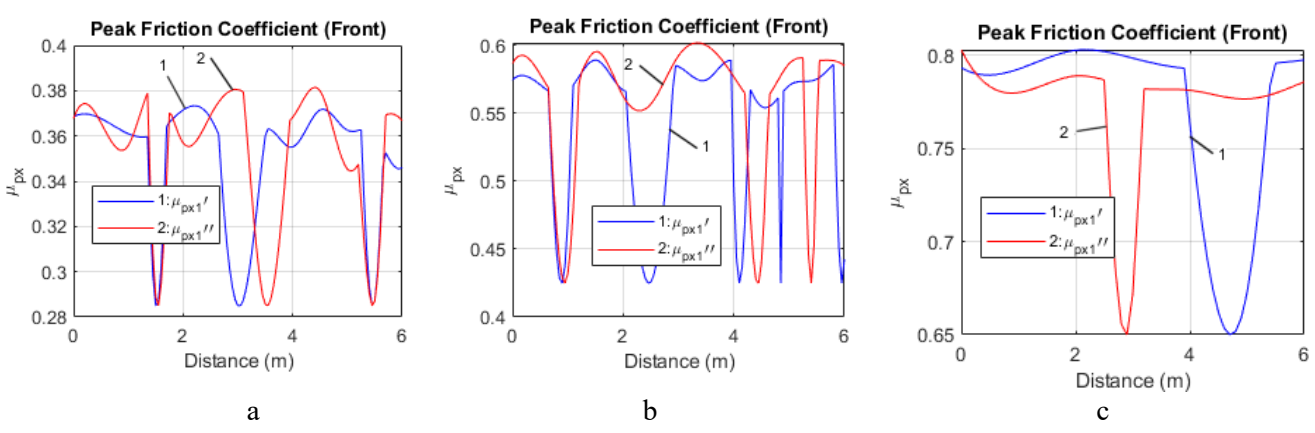


Fig. 2. Peak friction coefficient: a, b, c - soil, meadow, asphalt

In Fig. 3, the Velocity-based Mobility Performance Index is plotted for three terrains. Optimization of the gear ratio demonstrates potential to improve the mobility performance index on off-road terrain, especially on deformable soil. Mobility also has a small improvement on asphalt compared to the conventional driveline after optimization. Fig. 4 shows the actual velocities of the vehicles with the three drivelines. The increase of the velocity is the most on deformable soil (Fig. 4a).

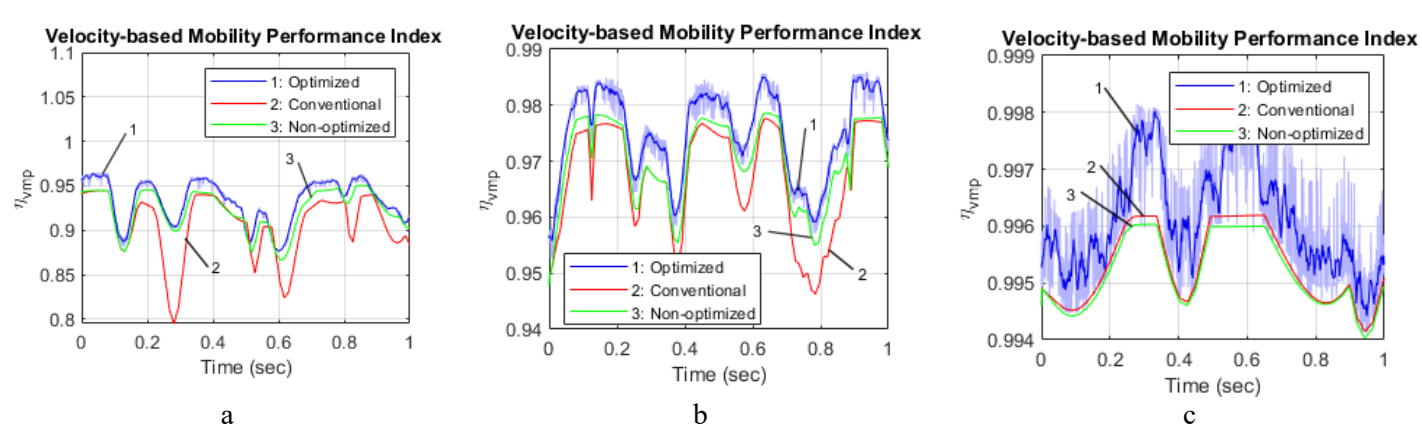


Fig. 3. Velocity-based Mobility Performance Index of the vehicle with three drivelines: a, b, c – soil, meadow, asphalt

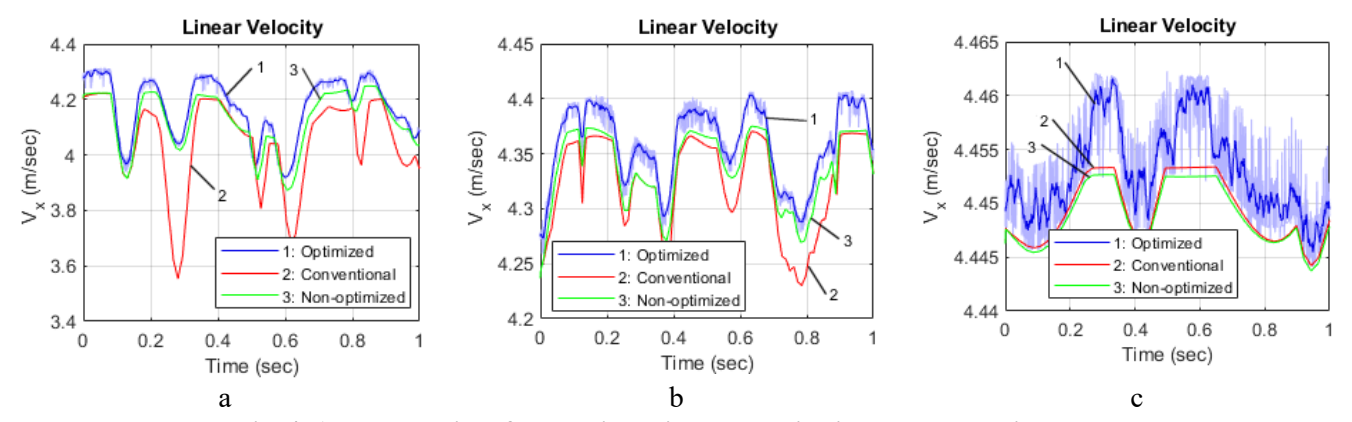


Fig. 4. Actual velocity of the vehicle with three drivelines: a, b, c – soil, meadow, asphalt

Fig. 5 provides data on the Wheel Mobility Indices (WMI) of all four wheels and the Vehicle Mobility Index (VMI) of the vehicle with three different drivelines when moving on soil terrain. The largest drop in WMI to below 0.3 is observed for the vehicle with the conventional driveline (Fig. 5b). In all other drivelines, the WMI and VMI is kept at appropriate high levels. The VMI values are high and provide suitable mobility margins with all three drivelines. The circumferential wheel forces, which result in slightly lower mobility margins, provide higher mobility performance of the vehicle with the optimized driveline as compared to the mobility performance of the vehicle with the conventional and non-optimized drivelines, as shown by its higher velocity on the same terrain. The optimized driveline can perform this function while always exceeding the mobility margin of the conventional driveline and avoiding severe drops in the mobility margin.

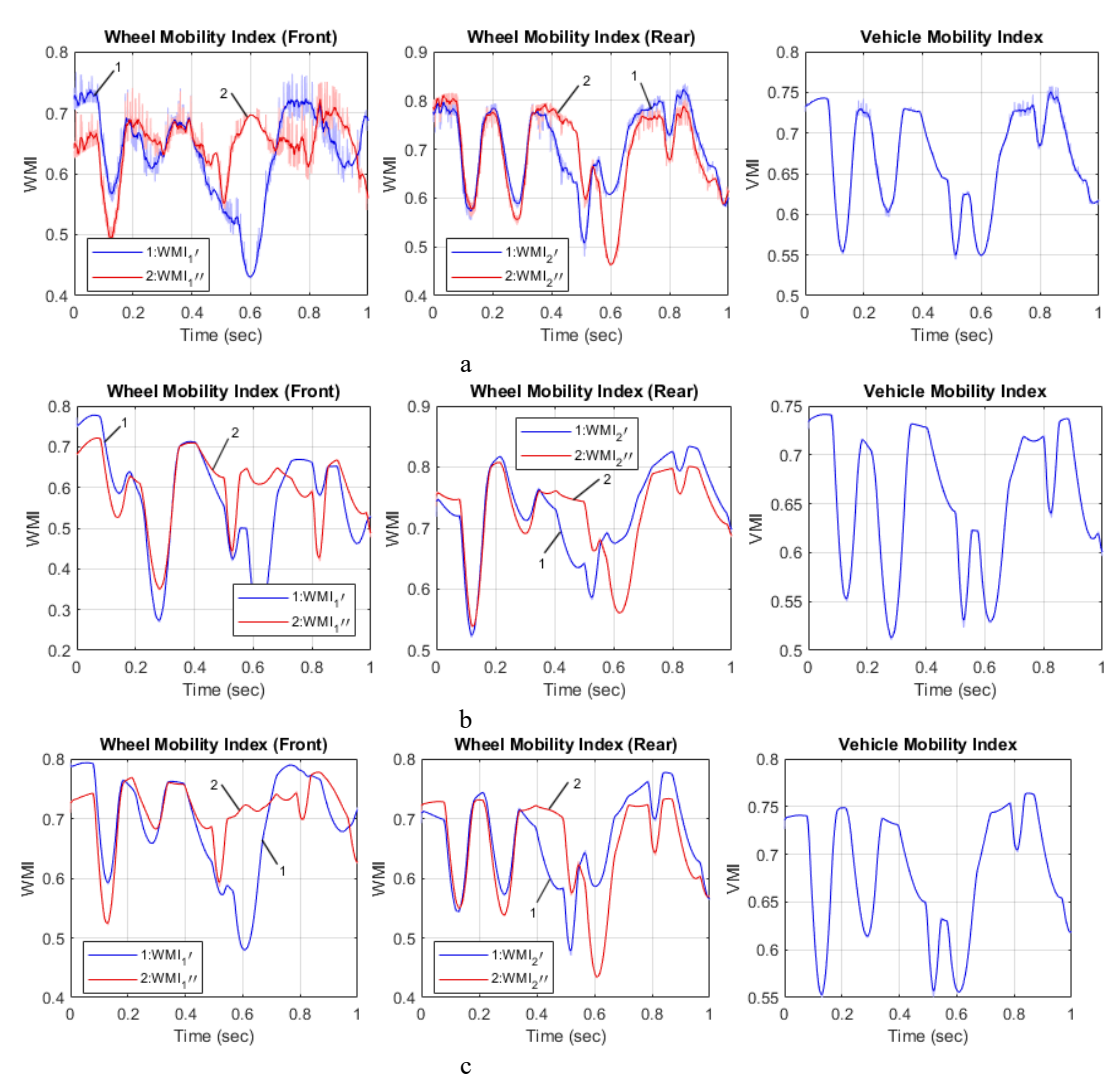


Fig. 5. Wheel Mobility Indices and Vehicle Mobility Index of the vehicle on soil terrain:

a, b, c - optimized driveline, conventional driveline, non-optimized driveline

Using the HE-PTU, the power transmitted to the wheels can be smoothly adjusted at all times, incorporating autonomy into the driveline systems of the vehicle. The mobility indices establish two factors to balance in the control of the AGV: assessing mobility performance and monitoring closeness to the immobilization status of the vehicle and its individual wheels. The next steps are development of an autonomous control that tracks mobility indices and adjusts the HE-PTU gear ratio in real time to maximize mobility performance within safe margins.

5 Conclusion

A 4x4 vehicle with a hybrid electric driveline including a controllable power split is studied for improving autonomous vehicle mobility. The controllable power split is achieved through the use of a hybrid electric power transmitting unit which provides a variable gear ratio. Two sets of mobility indices are presented for the purpose of (i) avoiding immobilization and (ii) improving velocity. The Wheel Mobility Index and Vehicle Mobility Index are suitable for assessing mobility margins of the wheels and the entire vehicle. The Velocity-based Mobility Performance Index was presented as a suitable index to assess mobility performance by comparing the actual velocity of a vehicle to the theoretical velocity of the same vehicle with a basic configuration of the driveline system. The mobility increase was accomplished while keeping the mobility margins at a high safe level. The next steps are developing an autonomous control that controls the mobility performance within safe margins.

Acknowledgments

This research was funded by the US Army CCDC Ground Vehicle Systems Center and partially by the National Science Foundation (award IIS-1849264)

References

- Thueer, T., Siegwart, R., Mobility evaluation of wheeled all-terrain robots. Robotics and Autonomous Systems, Robotics and Autonomous Systems 58(5):508-519, 2010. DOI: 10.1016/j.robot.2010.01.007.
- Ghotbi, B., González, F., Kövecses, J., Angeles, J., Mobility evaluation of wheeled robots on soft terrain: Effect of internal force distribution, Mechanism and Machine Theory, Volume 100, 2016, Pages 259-282, ISSN 0094-114X,
- 3. McCullough, M., Jayakumar, P., Dasch, J., Gorsich, D., The Next Generation NATO Reference mobility model development, Journal of Terramechanics, Volume 73, 2017, Pages 49-60, ISSN 0022-4898, https://doi.org/10.1016/j.jterra.2017.06.002.
- 4. Wong, J.Y., Jayakumar, P., Toma, E., Preston-Thomas, J., A review of mobility metrics for next generation vehicle mobility models, Journal of Terramechanics, Volume 87, 2020, Pages 11-20, ISSN 0022-4898, https://doi.org/10.1016/j.jterra.2019.10.003.
- Andreev, A.F., Kabanau, V.I., Vantsevich, V.V., Driveline Systems of Ground Vehicles: Theory and Design, V.V. Vantsevich, Scientific and Engineering Editor; Taylor and Francis Group/CRC Press, 792 pages, 2010.
- Vantsevich, V.V., Paldan, J., Gray, J.P., "A Hybrid-Electric Power Transmitting Unit for 4x4 Vehicle Applications: Modeling and Simulation", ASME 2014 Dynamic Systems and Control Conference, San Antonio, Texas, USA, 2014.
- Gray, J. P., Vantsevich, V.V., Overholt, J.L.. "Indices and Computational Strategy for Unmanned Ground Wheeled Vehicle Mobility Estimation and Enhancement" 2013 ASME 37th Mechanisms and Robotics Conference (MECH), Portland, OR, August 3-7, 2013.
- 8. Vantsevich, V., Gorsich, D., Paldan, J., and Letherwood, M., "A Virtual Driveline Concept to Maximize Mobility Performance of Autonomous Electric Vehicles," SAE Technical Paper 2020-01-0746, 2020 (in publication).